Dalton Transactions

Accepted Manuscript

ROYAL SOCIETY OF CHEMISTRY

www.rsc.org/dalton

TABLE OF CONTENTS entry

A macrocyclic ligand grafts on gold nanostars and binds Cu^{2+} not influencing the luminescence and photothermal properties of the nanoparticles

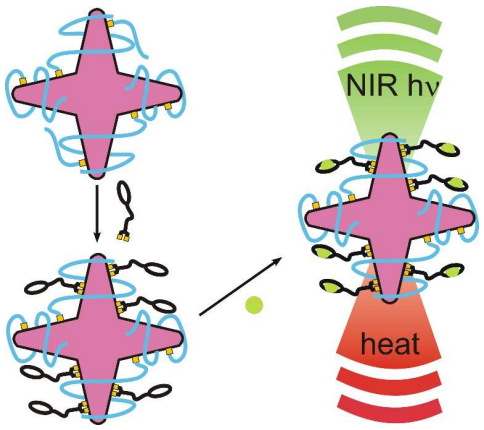

Journal Name

RSCPublishing

ARTICLE

Gold nanostars co-coated with the Cu(II) complex of a tetraazamacrocycle ligand

Cite this: DOI: 10.1039/x0xx00000x

Piersandro Pallavicini,*[a] Claire Bernhard,[b] Giuseppe Chirico,[c] Giacomo Dacarro,[a] Franck Denat,[b] Alice Donà,[a] Chiara Milanese[a] and Angelo Taglietti[a]

Received 00th January 2012,
Accepted 00th January 2012

DOI: 10.1039/x0xx00000x

www.rsc.org/

The twelve-membered tetraazamacrocylic ligand **L1** bears an appended lipoic acid unit, whose disulphide ring is an efficient grafting moiety for the surface of gold nanostars (GNS). The GNS that were used featured a localized surface plasmon resonance (LSPR) absorption at ~ 800 nm, *i.e.* in the near infrared (NIR). We investigated different approaches for coating them with the Cu^{2+} complex of **L1**. While the direct reaction of $[Cu\mathbf{L1}]^{2+}$ with as-prepared GNS led to aggregation, a first coating step with polyethyleneglycol-thiol (PEG-SH) was found to be advantageous. Displacement reactions were carried out on pegilated GNS either with $[Cu\mathbf{L1}]^{2+}$, directly generating $[Cu_n(\mathbf{L1}@GNS)]^{2n+}$, or with void **L1**, obtaining **L1**@GNS, that coordinates Cu^{2+} in a second step. In both cases, even with a large excess of the competing disulphide moiety, only partial displacement of PEG-SH is observed, obtaining ca 500-1500 $[Cu\mathbf{L1}]^{2+}$ per GNS depending on conditions, with PEG-SH remaining in the $[Cu_n(\mathbf{L1}@GNS)]^{2n+}$ hybrids and imparting them a remarkable stability. The photothermal and two-photon luminescence (TPL) properties of the GNS have been compared between the pegilated GNS and $[Cu_n(\mathbf{L1}@GNS)]^{2n+}$, finding that the grafted copper complex does not change them at any extent. Finally, the stability against demetallation and transmetallation of the complexes, as well as the fast kinetics of complexation of the monodispersed macrocycle and of **L1**@GNS have been examined, suggesting $[Cu_n(\mathbf{L1}@GNS)]^{2n+}$ as a device capable of TPL optical tracking and NIR photothermal therapy, and as a possible agent for PET imaging.

Introduction

Gold nanoparticles are very interesting objects in the nanomedicine area, due to their many peculiar physical-chemical properties.[1] They have been proposed as contrast-enhancing agents for computed tomography,[2] X-ray[3] and diffusion reflection[4] imaging applications. They also display efficient photothermal behaviour when irradiated at the wavelength of their LSPR, this property being particularly valuable when non-spherical gold nanoparticles are considered. In the latter case one or more LSPR bands fall in the near NIR region (750-1100 nm) in which water, blood and organic tissues are (semi)transparent. Non-invasive antitumor photothermal therapies have been envisaged[5] employing this kind of particles. Gold nanostars (GNS) are a category of non-spherical gold nanoparticles. Thanks to the easy control of their shape during syntheses and to the fine tuning of their optical properties (LSPRs span the 700-1600 nm range[6-11]) GNS are particularly promising for photothermal antitumor therapies, with some applications in this field already described by literature[12,13]. In addition, GNS can release active molecules upon short-pulse laser irradiation[14] and they are luminescent in the NIR range when irradiated on their LSPRs using the TPL technique.[15] The straightforward mix-and-obtain procedures[6-11] available for their surface functionalization with thiols add further appeal. The coating with –SH terminated polymers (e.g. polyethyleneglycol thiols, PEG-SH) enhances their stability, biocompatibility and allows in-vivo delivery.[16,6-8] Tunable co-coating with other functional -SH terminated molecules can be carried out, as we will show in this paper mixing PEG-SH with a remotely thiolated tetraaza macrocyclic Cu^{2+} complex.

Conjugation between metal complexes of macrocyclic ligands and nanoparticles is not a novelty, although it regards mainly small spherical nanoparticles (d<20 nm). Zn^{2+} complexes with a modified triazacyclononane decorating gold nanospheres were used as catalysts in transphosphorylation[17] and phosphodiester cleaving.[18] A Zn^{2+} porphyrin complex appended to gold nanospheres was tested as an efficient electrochemical sensor for anions.[19] Conjugates made of Gd^{3+} complexes with tetraazamacrocycles gathered on gold nanospheres have been

proposed as enhanced contrast agents in MRI (magnetic resonance imaging).[20,21]

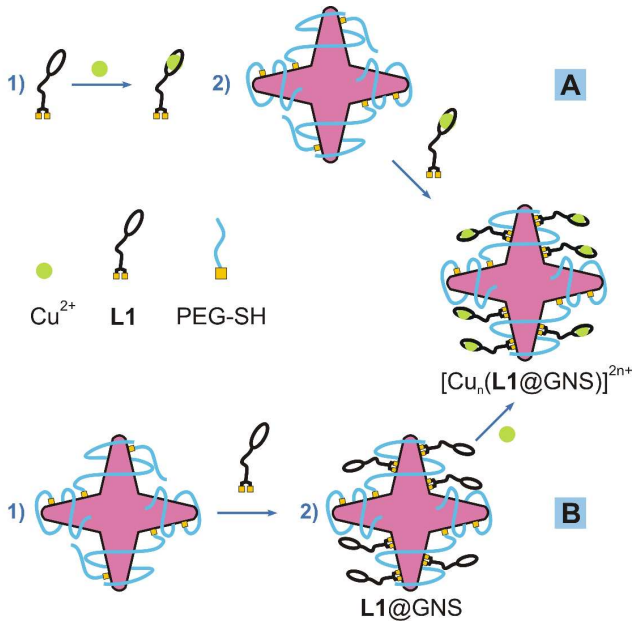

Fig 1 Sketch of the two approaches used to prepare GNS co-coated with $[CuL1]^{2+}$ and PEG-SH

Examples are reported in the literature also of tetraazamacrocycles of Cu^{2+} appended on nanoparticles and used in PET (positron emission tomography) imaging. A 14-membered macrocycle bearing three carboxylic acid groups on three of its amines,[22] a DOTA-like macrocycle (DOTA = 12-membered ring, bearing carboxylic acids on the four amino groups)[23] and a carboxylic acid functionalized macrobicycle[23] were conjugated on the surface of polymer core-shell nanoparticles, and their $^{64}Cu^{2+}$ complexes were formed and used to visualize the biodistribution of nanoparticles in mice. Modified DOTA-like tetraaza macrocyles were appended on the surface of Si-Mn[24] and Cd-Te[25] quantum dots, whose $^{64}Cu^{2+}$ complexes were able to target tumours in mice.[25] Some recent papers report grafting of DOTA derivatives to iron oxide nanoparticles, with their ^{64}Cu radiolabeled complexes that demonstrated to be suitable for multimodal imaging.[24-28] One example of gold nanocages surface-coated with $^{64}Cu^{2+}$ complexes with modified DOTA macrocycles has been also recently reported, using the ^{64}Cu radiolabelled agent to track the in-vivo pharmacokinetics of the gold nanocages.[29]

To the best of our knowledge, the conjugation of GNS with the metal complex of a tetraazamacrocycle is still unexplored. Moreover, the quantification of the average number of polymers and of co-coating molecules on the nanoparticles surface is a relatively poorly explored area, at least when large and non-spherical nanoparticles are considered, as in this case the use of standard NMR analytical techniques[30] is prevented by the high polydispersity and by the severe line broadening induced by the larger dimensions (e.g. 50-60 nm in our GNS case).[31,32] In addition, the influence of the d-d absorption bands and of the possible fluorescence quenching patterns[33] of a surface-grafted transition metal complex on the TPL and photothermal properties of GNS have never been ascertained. Within this framework, we present here the synthesis of the twelve-membered tetraazamacrocylic ligand **L1,** bearing an appended lipoic acid unit as a grafting moiety for the surface of GNS (see Scheme 1). With this, we introduce two approaches to obtain $[CuL1]^{2+}$-coated GNS, namely $[Cu_n(L1@GNS)]^{2n+}$: the first is the single-step reaction of pegilated GNS with $[L1Cu]^{2+}$ (Figure 1A), the second is the reaction of void **L1** with pegilated GNS, to give **L1**@GNS, followed by Cu^{2+} complexation (Figure 1B). A method for the determination of the surface composition of the obtained products is also presented, using a combination of ICP-OES and thermogravimetric analysis (TGA). Proofs of the null effect exerted by the grafted $[CuL1]^{2+}$ complex on the photothermal and luminescence properties of GNS are given. Finally, although only at a proof of concept level, the possible use of the $[Cu_n(L1@GNS)]^{2n+}$ hybrids in PET has been investigated by examining the Cu^{2+} complexation kinetics both in monodispersed ligands and in **L1**@GNS, and by checking the complexes stability towards demetallation in acidic conditions and towards competitive exchange with bio-available cations like Na^+, Ca^{2+}, Fe^{2+} and Zn^{2+}.

Experimental

All the used reactants, solvents and instruments are listed in the ESI. The synthesis of the starting compounds **1-3** (Scheme 1) and of activated lipoic acid are described in the ESI. Experimental details on complexation kinetics, demetallation and transmetallation tests on ligand **L2** are also described in the ESI.

5-(1,2-Dithiolan-3-yl) – *N* - (2 - (2 - (4,7,10 – trimethyl - 1,4,7,10 – tetraazacyclododecan – 1 -yl) acetamido) ethyl) pentanamide (**L1**). The carboxylic group of lipoic acid was activated with N,N'-disuccinimidyl carbonate. 594 mg of **3** (0.00189mol) and 572 mg of the activated lipoic acid (0.00189mol) were dissolved in 70mL of CH_3CN. The mixture was stirred overnight at room temperature. The solvent was evaporated to give a yellow oil. The oil was dissolved in dichloromethane and washed with NaOH 2M. The organic phase was dried over $MgSO_4$. The solvent was evaporated on a rotary evaporator to give **L1** as a yellow oil (886mg, 0,00176mol, yield = 93.3%). MALDI-TOF : 503.016 $(L1+H)^+$. ^1H NMR (300 MHz, $CDCl_3$, 300K). δ (ppm): 1.30 (m, 2H, CH_2), 1.51 (m, 4H, CH_2), 1.80 (m, 1H, CHS), 1.97 (s, 9H, CH_3), 2.03 (m, 4H, CH_2), 2.29 (m, 14H, CH_2, CH_2NH), 2.98 (m, 4H, CH_2, CH_2S), 3.19 (t, 2H, CH_2CO), 3.42 (broad s, 2H, NCH_2CO), 5.18 (2H, CH_2NH), 7.09 (s, 1H,NHCO), 9.62 (s 1H, NHCO).

1,4,7-Trimethyl-10-propyl-1,4,7,10-tetraazacyclododecane (**L2**). In a 250mL flask, 700mg (0.00327 mol) of **1** were dissolved in 40mL of dichloroethane. 900mg of sodium triacetoxyborohydride were added and solubilized (0.004251 mol, 1.3 eqv). 190mg of propionaldehyde (0.00326 mol) dissolved in 20mL of dichloroethane were added slowly under

stirring and nitrogen atmosphere. After 3 days, 100mL of NaOH 1M and 50 mL of chloroform were added to the mixture. The aqueous phase was extracted with 3×100mL of chloroform. The organic phase was dried over $MgSO_4$ and the solvent evaporated to give 600mg of a dark yellow oil. The oil was purified with the addition of 50mL of diethyl ether. After 10 min, the mixture was filtered on celite and the solvent evaporated to give **L2** as a yellow oil (485mg, 0.00190mol, yield = 58.1%). **^{1}H NMR** (300 MHz, $CDCl_3$, 300K). δ (ppm): 0.23 (t, 3H, J=7.4Hz), 0.82 (q, 2H, J=7.4Hz), 1.75 (m, 27H). **ESI-MS**: 257.3 (**L2**+H)$^+$.

[CuL1](CF$_3$SO$_3$)$_2$. 352 mg (0.70 mmol) of **L1** were dissolved in 8 mL of ^{t}BuOH and 0.7mL of a $Cu(CF_3SO_3)_2$ 1.0 M aqueous solution were added. Water (0.5 mL) was added to obtain complete solubilisation. The mixture was heated at reflux for 1h. Precipitation of the complex as a blue powder was obtained with the addition of diethyl ether. **MS-ESI:** 282.9 $(C_{23}H_{46}CuN_6O_2S_2)^{2+}$; 564.5 $(C_{23}H_{46}CuN_6O_2S_2 - H)^+$; 714.2 $(C_{23}H_{46}CuN_6O_2S_2 + CF_3SO_3)^+$.

[CuL2](CF$_3$SO$_3$)$_2$. 24.6mg (0.096 mmol) of **L2** were dissolved in 5mL of ^{t}BuOH and 96.1µL of an aqueous solution of $Cu(CF_3SO_3)_2$ 1M were added. Water (0.2mL) was added to obtain complete solubilisation. The mixture was heated at reflux for 1h. The precipitation of the complex as a blue powder was obtained with the addition of diethyl ether. **MS-ESI:** 159.7 $(C_{14}H_{32}CuN_4)^{2+}$; 319.3 $(C_{14}H_{32}CuN_4 - H)^+$; 468.1 $(C_{14}H_{32}CuN_4 + CF_3SO_3)^+$.

Gold nanostars and GNS coating with PEG-SH. Fresh GNS solutions were prepared following a procedure already described by us,[7,8] see ESI for details. Coating with PEG-SH was carried out by adding PEG-SH in 5×10^{-5}M concentration. The solution was stirred for 2h at room temperature and purified with two cycles of ultracentrifugation (13000 rpm, 25 min), supernatant discard and redissolution of the GNS pellet in bidistilled water (10 mL).

Preparation of $[Cu_n(\mathbf{L1}@GNS)]^{2n+}$ ($CF_3SO_3^-$ salt) by reaction of $[Cu\mathbf{L1}]^{2+}$ ($CF_3SO_3^-$ salt) with pegilated GNS. In a typical synthesis, a concentrated solution of *$[Cu\mathbf{L1}](CF_3SO_3)_2$* is added to 30 ml of pegilated GNS, reaching the desired final concentration (10^{-4} M or 10^{-3}M). The mixture is allowed to react at the chosen temperature (room temperature i.e. 25 °C, or 60°C) for 1h. The GNS were then ultracentrifugated (13000rpm, 25 min) the supernatant discarded and the pellet re-dissolved in bi-distilled water. Four different combinations of concentration and temperature were tested, as shown in Table 1. For the quantitative determination of the grafted Cu^{2+} complexes (see Figure 2B and Table 2), 25 mL of the solution were divided into 5 portions of 5.0 mL, that underwent 1, 2, 3, 4 and 5 cycles of centrifugation / supernatant discarding / redissolution, respectively. The final pellet was redissolved in water, oxidized with 3.0 ml aqua regia and analysed with ICP-OES.

*Two-steps preparation of $[Cu_n(\mathbf{L1}@GNS)]^{2n+}$ ($CF_3SO_3^-$ salt): synthesis of **L1**@GNS and its complexation with Cu^{2+} (as $CF_3SO_3^-$ salt)*. In a representative preparation, a concentrated solution of chelator **L1** was prepared, containing 0.2M LSB to promote solubility. This solution was added to 30mL of the pegilated GNS solution, reaching the desired final concentration of **L1**: 10^{-4} M, 10^{-3} M, 10^{-2} M. The mixture was allowed to react at room temperature (25°C) for 2h, then it underwent two cycles of ultracentrifugation (13000rpm, 25min)/supernatant discarding/redissolution of the pellet in bidistilled water (30mL). This is a solution of **L1**@GNS, that was then treated with excess $Cu(CF_3SO_3)_2$ (reaching an equimolar quantity of Cu^{2+} with respect to total **L1** added in the previous step) and allowed to react for 1 hour at 60 °C. The same preparation was carried out with three different concentrations, as summarized in Table 1. For Cu^{2+} quantitative determination (see Table 3), GNS underwent three cycles of ultracentrifugation/redissolution, with supernatant discard. The final GNS pellet was then redissolved in 3.0 mL aqua regia and Cu^{2+} analysed by ICP-OES.

For the complexation experiments run with the quantity of Cu^{2+} commisurate to the void **L1** ligands actually grafted on GNS, we used two conditions (see Table 1): a) **L1** 10^{-4} M and all steps as described until the attainment of **L1**@GNS solution. Then, on a 10 mL portion of this solution, a $Cu(CF_3SO_3)_2$ solution was added up to a final concentration of 0.9×10^{-6} M (this quantity is calculated as the 60% of the grafted $[Cu\mathbf{L1}]^{2+}$ found by ICP-OES in the already described procedure, with 10^{-4} M **L1**). The solution was allowed to react at 60 °C for 1 hour, then it underwent two ultracentrifugation/supernatant discard/redissolution cycles. A 5 mL portion of the final solution was treated with aqua regia and then analysed by ICP-OES. b) Same, with **L1** 10^{-3} M and final Cu^{2+} concentration: 1.14×10^{-6} M.

Table 1.Synthetic parameters for the preparation of $[Cu_n(\mathbf{L1}@GNS)]^{2n+}$

One-step		Two-steps			
$[Cu\mathbf{L1}]^{2+}$ (mol/L)	T (°C)	[**L1**] (mol/L)	T1[a] (°C)	[Cu] (mol/L)	T2[a] (°C)
10^{-4}	25	10^{-4}	25	10^{-4}	60
10^{-4}	60	10^{-3}	25	10^{-3}	60
10^{-3}	25	10^{-2}	25	10^{-2}	60
10^{-3}	60	10^{-4}	25	$0.9*10^{-6}$ [b]	60
		10^{-3}	25	$1.14*10^{-6}$ [b]	60

[a] T1 and T2 in the two-steps procedure are the temperature of reaction with L1 (T1) and of Cu^{2+} complexation on void **L1**@GNS (T2); [b] 60% of the Cu^{2+} concentrations determined by ICP-OES experiments (Table 3) in $[Cu_n(\mathbf{L1}@GNS]^{2n+}$ prepared from **L1**@GNS with excess Cu^{2+}.

Results and discussion

1. Strategy for ligand preparation. The synthetic strategy is described in Scheme 1. Ligand **L1** has been obtained from **1**, a building block made of a 12aneN4 macrocycle methylated on three of its four amino groups. Trimethylation leaves only one secondary amine available for further functionalization, allowing to obtain **L1,** which bears a single remote disulphide group for grafting on the surface of GNS. A single grafting point per ligand is a desired requirement, as it prevents the possibility of bridging between two or more different nanoparticles, which would lead to aggregation. **L1** is obtained from **1** in three steps, first reacting **1** with the stoichiometric

quantity of ethylbromoacetate to yield **2**. Reaction of the latter with a ten-fold excess of ethylenediamine gives **3**, which is finally coupled with a stoichiometric quantity of activated lipoic acid to give **L1**. Lipoic acid (**LA**, Scheme 1) has been chosen as the grafting unit instead of the frequently used α-mercapto ω-carboxylic acids. The choice is based on two reasons: first the -S-S- moiety is stable and oxidative dimerization of –SH groups during or post-synthesis is ruled out; second, the endocyclic disulphide unit forms particularly stable monolayers on spherical gold[34-35] nanoparticles, thanks to the formation of two thiolate-Au(I) bonds per molecule, exerting a sort of chelate effect on the surface (see **LA**@Au, Figure 1) that disfavours detachment.[36] Finally, **1** has been also used to prepare the reference ligand **L2** with a one-step reductive amination with propionaldehyde, in the presence of sodium triacetoxy borohydride.

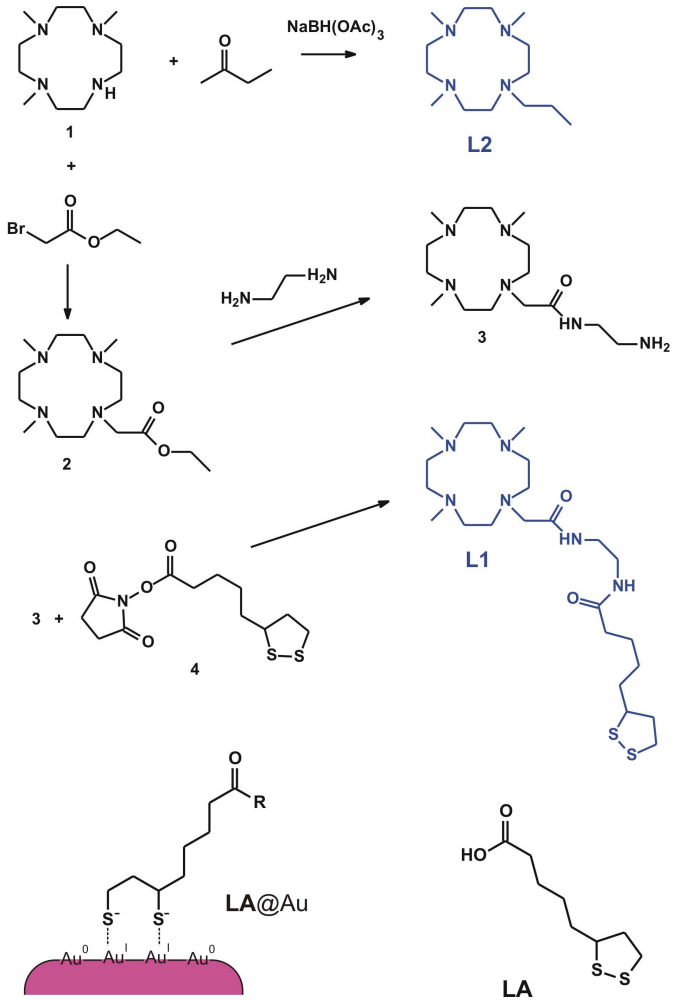

Scheme 1. Synthetic chart and formula for ligands **L1** and **L2**

2. Grafting [CuL1**]$^{2+}$ on GNS**. Gold nanostars were prepared as described in our previous papers.[7,8] Their seed-growth synthesis uses laurylsulfobetaine (LSB) as the protecting and directing agent. Besides some undeveloped spheres, the synthesis yields aqueous colloidal solutions containing a mixture of monocrystalline GNS as the minor product (20-30%, Figure 3A, inset i), and pentatwinned irregularly branched GNS as the major product (60-70%, Figure 3A, inset ii). The aspect ratio (AR) of the branches of monocrystalline GNS is poorly influenced by the synthetic conditions, with an LSPR band always centred at 650-700 nm. The AR of the branches of pentatwinned GNS and the relative LSPR absorption can be finely tuned by regulating the reactants concentration (650nm < λ_{max} <1150nm). In all the preparations for this paper we have adopted the same reaction conditions, leading to GNS with absorption spectra as exemplified in Figure 2A. The main LSPR band is centred in the 800-830 nm range to match with the wavelength of our NIR laser source (800 nm) for photothermal use. After the growth process, 10 mL portions of GNS solutions were ultracentrifuged and redissolved in 10 mL bidistilled water. These are our starting colloidal solutions for coating procedures. Most of the excess LSB present in solution is removed with this protocol, with a weakly bound double layer of LSB remaining on the surface of the GNS, imparting them a negative Z potential: this double layer is easily removed and the GNS are coated with thiols by simple addition of RSH to their aqueous solutions.[7,16] Accordingly, our first attempt was to prepare GNS fully coated with [Cu**L1**]$^{2+}$ (the complex has two $CF_3SO_3^-$ as the counter anions, omitted for sake of graphical simplicity).

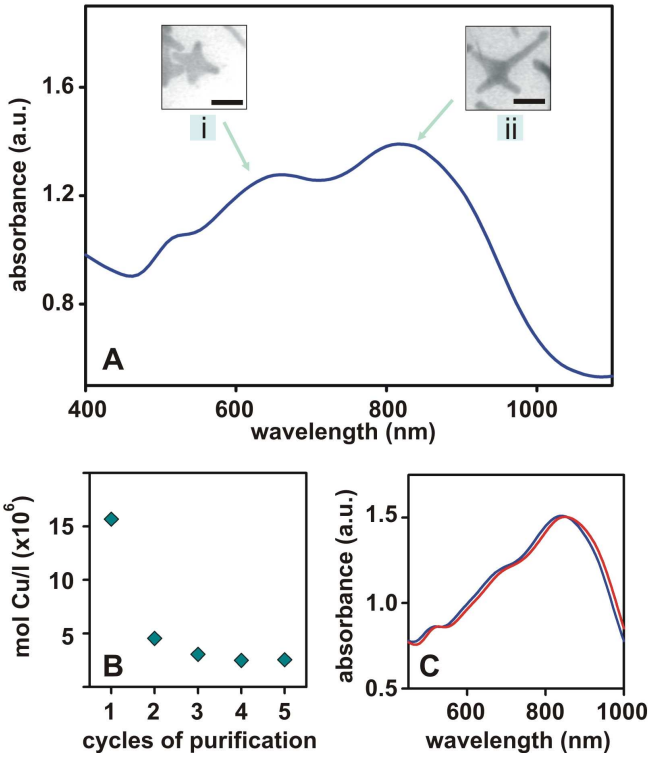

Fig 2 **A**: representative absorption spectrum of a GNS solution at the end of the seed-growth synthesis in LSB. Insets: TEM images of the GNS typology responsible of the LSPRs: (ii) = pentatwinned irregularly branched GNS, (i) = monocrystalline GNS, scale bars = 25 nm. **B**: copper concentration in a solution of [Cu$_n$(**L1**@GNS)]$^{2n+}$ prepared by exchanging PEG-SH with 10^{-3} M [Cu**L1**]$^{2+}$ (60 °C)

vs purification cycles. **C**: absorption spectrum of a solution of GNS coated with PEG-SH (blue); same solution after treatment with 10^{-3} M [Cu**L1**]$^{2+}$ (60°C) for 1 hour (red)

The copper complex of **L1** was added to a solution of GNS (10 mL, total Au = 3.75×10^{-4} mol/L) in one portion to reach 5×10^{-5} M concentration. At this concentration the grafting molecules are in a $2x10^4$ molar ratio with respect to GNS (average GNS concentration is 2.4×10^{-9} mol/L, see ESI). As we have already shown[7,8] at such a ratio the maximum possible surface coating with R-SH is obtained in less than one hour. However, degeneration of the absorption spectra due to fast aggregation and precipitation of GNS was observed with this procedure (see ESI, Figure S1). Also the reverse approach, i.e. the addition of a small sample of GNS solution to a 5×10^{-5} M solution of [Cu**L1**]$^{2+}$, lead to GNS aggregation. This is probably caused by the slow advancement of the adhesion process of [Cu**L1**]$^{2+}$ to the GNS surface, leading after few minutes to partial coating. While the surface charge of freshly prepared GNS is negative (Z = -15 mV) the added copper complex is positive (+2 or +1 depending on pH, vide infra). Partial coating leads to neutral surface charge and promotes aggregation. We thus changed approach, first fully coating GNS with a stabilizing polyethyleneglycol-thiol polymer, (PEG-SH, average MW 2000) and then partially exchanging PEG-SH with [Cu**L1**]$^{2+}$, as sketched in Figure 1A. GNS were pegilated as already described,[8] with two ultracentrifugation/redissolution cycles after pegilation, in order to eliminate adventitious LSB from the product.[7] The solutions of pegilated GNS were then treated with 10^{-3} or 10^{-4}M [Cu**L1**]$^{2+}$ at 25°C or 60°C (1h) to obtain the displacement reaction leading to [Cu$_n$(**L1**@GNS)]$^{2n+}$ ($CF_3SO_3^-$ counteranions omitted from the trivial name for simplicity). It has to be stressed that the surface-grafted PEG-SH is only partially replaced by [Cu**L1**]$^{2+}$ during the displacement process (vide infra for quantification in a representative case). This brings advantages, as the remaining grafted PEG-SH imparts stability against aggregation and it is necessary in the perspective of *in-vivo* use of the hybrids, due to PEG's "stealth" effect on nano-sized drug carriers and contrast agents.[37,38] The [Cu$_n$(**L1**@GNS)]$^{2n+}$ hybrids can be ultracentrifuged and redissolved in water repeatedly, with no degradation. This allowed to determine the exact content of Cu^{2+} grafted on the GNS. 25 mL solutions of [Cu$_n$(**L1**@GNS)]$^{2n+}$, prepared with 10^{-3} or 10^{-4}M [Cu**L1**]$^{2+}$ (1h, 25°C or 60°C) were divided into 5 portions of 5.0 mL each.

Table 2 Concentration of grafted [Cu**L1**]$^{2+}$ (mol/L) in the prepared [Cu$_n$(**L1**@GNS)]$^{2n+}$ solutions, surface number per GNS and Z potential of [Cu$_n$(**L1**@GNS)]$^{2n+}$, obtained by exchange with [Cu**L1**]$^{2+}$ on pegilated GNS

starting [Cu**L1**]$^{2+}$ (mol/L)	T (°C)	Cu (mol/L)	average number of [Cu**L1**]$^{2+}$/GNS	Z (mV)
10^{-4}	25	7.6×10^{-7}	304	+4 (1)[a]
10^{-4}	60	1.6×10^{-6}	640	+7.6 (0.7)[a]
10^{-3}	25	2.7×10^{-6}	1080	+20(3)[a]
10^{-3}	60	2.7×10^{-6}	1080	+14 (4)[a]

[a] uncertainties in parenthesis. The pH of the colloidal solution was in the 6.0-6.5 range after the displacement reaction. At this pH the copper complex with 12aneN4 is 100% in its [Cu^{2+} (H_2O)] form, bearing a +2 charge

These portions underwent a different number of ultracentrifugation/redissolution purification cycles, from 1 to 5, after which copper content was determined by ICP-OES. Purification cycles eliminate any copper complex adventitiously adsorbed on the GNS surface and the excess complex dissolved in the small portion of solution imbibing the centrifuged pellet. Cu^{2+} concentration plotted against the number of purification cycles shows a decrease-plateau trend, readily getting to a constant value at the second cycle, Figure 2B. Displacement of PEG-SH by [Cu**L1**]$^{2+}$ has been carried out under the four mentioned combinations of concentration and temperature (see Table 1). The plateau values were considered as the actual concentrations of Cu grafted on GNS, expressed in mol/L, and are summarized in Table 2. By increasing the [Cu**L1**]$^{2+}$ concentration in the displacement reaction, an increase of the grafted complexes is obviously found. On the other hand, increasing the temperature from 25 to 60 °C resulted in an increase of the grafted complex only in the experiments at the lower concentration (10^{-4} M [Cu**L1**]$^{2+}$), while at the highest concentration of [Cu**L1**]$^{2+}$ (10^{-3} M) the values were identical at the two temperatures. This suggests that the maximum possible surface concentration is reached only when using 10^{-3} M [Cu**L1**]$^{2+}$. In the case of 10^{-4} M [Cu**L1**]$^{2+}$, a kinetic effect could be present, promoting faster exchange at higher temperature. However, we did not further investigate neither the kinetics nor the maximum possible surface concentration attainable by this approach. If a possible use of these hybrids will be envisaged in the future for PET imaging, using Cu radionuclides, preparing first the Cu^{2+} complex of **L1** and then grafting it on GNS would be a time consuming and somewhat tricky two-step procedure, that could be undesirable with the relatively short living radioactive ^{64}Cu isotope (half-life 12.7 h). We consider this part of the research as a proof of concept, necessary to demonstrate the existence of [Cu$_n$(**L1**@GNS)]$^{2n+}$ and to investigate its features.

Characterization [Cu$_n$(**L1**@GNS)]$^{2n+}$ was carried out by UV-Vis absorption spectroscopy, Z-potential measurements and TEM imaging, see Table 2. A red shift of ~7 and ~10 nm of the LSPR bands was observed for treatments with 10^{-4}M and 10^{-3}M [Cu**L1**]$^{2+}$, respectively, due to the change in composition of the surface coating. Besides this shift, LSPR bands do not change in shape, Figure 2C, indicating that no aggregation or GNS morphological modification takes place with the PEG-

SH/[Cu**L1**]$^{2+}$ co-coating. This is also confirmed by TEM images taken on pegilated GNS and on the same product after treatment with [Cu**L1**]$^{2+}$ (ESI, Figure S2). The Z potential shows the expected change to positive values, due to the +2 charge of the copper complex (slightly acidic pH values, 5.8-6.2, are observed after the grafting process: section 3 further discusses the copper complex composition and charge *vs* pH). The higher Z values found after the 10^{-3} M displacement reaction is coherent with the higher Cu^{2+} concentration on the GNS surface. A control experiment was carried out by adding the Cu^{2+} complex of chelator **L2** to a GNS solution, at 10^{-3} M concentration. **L2** has no function capable of grafting on GNS and coherently, no change was observed in the absorption spectrum and in the Z potential of the pegilated GNS, demonstrating that what is observed with [Cu**L1**]$^{2+}$ is the actual grafting of the disulphide function on gold and not an electrostatic interaction between the positively charged copper complex and the negatively charged GNS.

3. Evaluation of the quantity of PEG-SH and [CuL1]$^{2+}$ in pegilated GNS and in [Cu$_n$(L1@GNS)]$^{2n+}$. In order to finely understand the entity of PEG-SH displacement and the nature of the GNS mixed coating, it is important to evaluate not only the total solution concentrations of Cu^{2+} grafted on the GNS surface, but also the number of [Cu**L1**]$^{2+}$ complexes actually grafted on a single nanostar. The GNS solution is a two-component mixture, i.e. two nanostars typologies coexist, regular six-branched monocrystalline and pentatwinned.[7,8] The latter is largely predominant and the number of branches protruding from the central pentatwinned core varies from one to five. The width and length of the branches, the number of branches per GNS in the case of pentatwinned nanostars, and the diameter of the GNS core can be measured from TEM images (see ESI, Figure S3) and their average values calculated. We used a geometrical model of the GNS shape, consisting of a spherical core and six conical branches (monocrystalline regular nanostars) or three conical branches (average branches number in the case of pentatwinned nanostars), see ESI. From the calculated volume and considering Au density, an average mass of 5×10^{-17} g is calculated for a single GNS, for both monocrystalline and pentatwinned typology. The identical value is a coincidence due to the different branches dimensions and to the different number of branches in the two cases. The transformation yield of Au(III) into GNS is 75% under the used experimental conditions (ESI). From the mass of a single GNS and from the concentration of gold transformed into GNS, the molar concentration of GNS objects in solution is obtained (2.45×10^{-9} M, ESI for details). Finally, from the ratio between the [Cu**L1**]$^{2+}$ molar concentrations of Table 2 and this value, the average number of copper complexes per single GNS is calculated and also listed in Table 2. Quite interestingly, calculated numbers are very close or even higher than those found in our previous studies for the number of PEG-SH molecules (mw 2000) coating a single GNS (750).[7,8] According to this, the values of Table 2 may apparently suggest that PEG-SH is entirely displaced by [Cu**L1**]$^{2+}$ on the GNS surface. However, we observed that even at the highest surface concentration of [Cu**L1**]$^{2+}$ the hybrid [Cu$_n$(**L1**@GNS)]$^{2n+}$ maintains a remarkable stability against aggregation, e.g. during stressing ultracentrifugation/redissolution procedures. This is compatible only with a high number of PEG-SH molecules remaining grafted on the GNS surface, a consideration that led us to formulate the hypothesis of only partial PEG-SH displacement, as pictorially described in Figure 1A.

To demonstrate this, we run DSC measurements. We scaled up the preparation of pegilated GNS to a total volume of 200 mL. Half of this sample was treated with 10^{-4} M [Cu**L1**]$^{2+}$ at 60 °C. From both samples we separated the coated GNS after two cycles of ultracentrifugation/ supernatant discarding / redissolution, obtaining a dry pellet of ~ 7 mg after vacuum drying. A 3.5 mg sample of each was analysed by DSC (profiles are included in the ESI, Figure S4). In the case of pegilated GNS, a single sharp endothermic peak at ~ 50 °C is observed, due to the melting of PEG-SH. By comparing the melting enthalpy of the pure PEG-SH (155.9 J/g, determined by an independent experiment) with the value measured on the coated GNS (7.67 J/g) the PEG-SH mass amount is estimated 4.92%. Such a weight % corresponds to 780 PEG units/GNS (ESI for calculation), in agreement with the 750 value found in our previous studies.[7] When the calorimetric profile of the [Cu$_n$(**L1**@GNS)]$^{2n+}$ hybrids is examined, two sharp endothermic peaks are observed, one at 50 °C due to PEG-SH and a new one, at ~ 250 °C, due to the grafted [Cu**L1**]$^{2+}$ complex. The peak of PEG-SH corresponds to 3.79 % in weight. By merging this with the Cu^{2+} concentration obtained by ICP-OES on the same solution, 1.75% weight is found for [Cu**L1**](CF$_3$SO$_3$)$_2$ grafted on GNS (see ESI for detailed calculation). The decrease of PEG-SH % weight and the % weight of the grafted copper complex fits with the partial displacement that we hypothesized on the basis of [Cu$_n$(**L1**@GNS)]$^{2n+}$ stability. Moreover, from the % weight data a number of 602 PEG-SH and 645 [Cu**L1**]$^{2+}$ per GNS are calculated (details in the ESI), the latter fitting very well with the number found with ICP-OES analysis reported in Table 2.

According to these data, the displacement process on the coating PEG-SH layer of GNS should be better described as the [Cu**L1**]$^{2+}$ molecules (or empty **L1** molecules, see next section) *adding* on the GNS surface and *only partially* displacing the PEG-SH polymers, as pictorially described in Figure1A, this leading to the hypothesized co-coating. Reassuringly, this also agrees with our previous observation that PEG-SH coating increases only slightly the average hydrodynamic radius of GNS, observed with dynamic light scattering,[15] indicating that PEG-SH molecules graft on GNS and wrap around it, leaving a large portion of the GNS surface free for further Au-thiol interactions.

4. Grafting L1 ligand on GNS and subsequent Cu^{2+} complexation. The data obtained in the previous section, demonstrating the mixed surface composition and the consequent stability of the [Cu$_n$(**L1**@GNS)]$^{2n+}$ hybrid, prompted us to use a second approach, depicted in Figure 1B. Void ligands are first grafted on pegilated GNS, with only

partial displacement of PEG-SH, to obtain **L1**@GNS. When this receptor is purified by repeated ultracentrifugation/redissolution cycles it is ready to quickly incorporate Cu^{2+} in the 12aneN4 cavity by complexation in aqueous solution. As it will be shown in this section, we consider this approach more convenient with respect to the preceding one as it would cut the workup duration after Cu^{2+} addition and allow all the added Cu^{2+} to be bound to GNS. Both aspects might be of primary importance when using short-living copper radionuclides, e.g. for PET imaging.

We first studied the kinetic profile of the complexation of Cu^{2+} with the model ligand **L2** that has the same donor set as **L1**. It is known that complexation of metal cations in N-methylated tetraaza macrocyclic ligands may have a first fast step followed by a second slower rearrangement.[39] In need of fastening the complexation process, in the perspective of using these materials for $^{54}Cu^{2+}$ incorporation, we examined the kinetics of the reaction at 60 °C. Spectra were collected every 90 sec for the first 30 minutes and then every 300 sec. The series is displayed in Figure 3A. The $[Cu\mathbf{L2}]^{2+}$ complex displays an intense CT band at 290 nm (ε = 3900 M^{-1} cm^{-1}) and a d-d transition at 604 nm (ε = 375 M^{-1} cm^{-1}). The inset of Figure 3A shows an enlargement of the final spectrum in the d-d band range. Figure 3B displays the plot of the absorbance at 290 nm and at 604 nm vs time, showing that the process goes to completion in ~ 60 minutes.

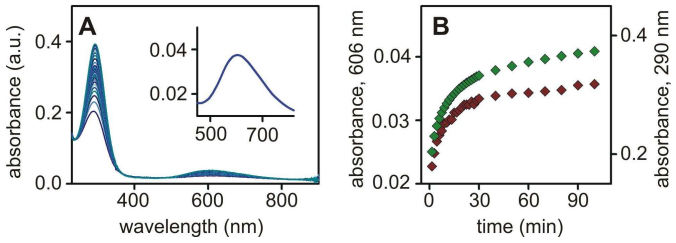

Fig 3 A: absorption spectra for **L2** complexation with $Cu(CF_3SO_3)_2$ (60 °C, **L2** and metal cation 10^{-4} M), t = 0-100 min (bands at 290 and 604 nm increase with time). Inset: enlargement of 500-800 range for the 100 min spectrum, evidencing the d-d band. **B**: absorption at 604 nm (dark red diamonds, left vertical axis) and at 290 nm (green diamonds, right vertical axis) for the spectra displayed in **A**

The inset of Figure 3A shows that the d-d absorption has a maximum position and a band shape nearly identical to what found for Cu^{2+} with the analogous N,N',N''-trimethyl-N'''-dodecyl-12aneN4 ligand,[40] indicating a square pyramidal geometry for Cu^{2+} with the N4 donor set at the basis and the apical position occupied by a water molecule.[41] This kind of complexes are subject to deprotonation of the apically coordinated water molecule with a pKa value of 7.65 for the aforementioned dodecylated 12aneN4 ligand.[40] In the case of **L2**, the equilibrium between $[Cu(\mathbf{L2})H_2O]^{2+}$ and $[Cu(\mathbf{L2})OH]^{+}$ was studied with a spectrophotometric titration, finding an absorbance change corresponding to a pKa of ~ 7.7 (see ESI, Figure S5-S6): the absorption spectra of the d-d transition subtly changes between $[Cu(\mathbf{L2})H_2O]^{2+}$ and $[Cu(\mathbf{L2})OH]^{+}$,with the maximum shifting from 604 to 609 nm and the band displaying an increased shoulder at longer wavelengths. The well-known kinetic inertness of the complexes of tetraazamacrocycles was tested against protonation and demetallation by dissolving $[Cu\mathbf{L2}]^{2+}$ in 0.1M $HClO_4$. No spectral changes were observed in 24 hours at 60 °C. Moreover, as a first indication of a possible in vivo use, inertness against displacement by competing cations that may be found in the human body was also verified. A 10^{-4} M aqueous solution of $[Cu\mathbf{L2}]^{2+}$ was treated with ten-fold excess of Zn^{2+}, Fe^{2+}, Na^{+} (triflate salts) and Ca^{2+} (chloride salt). No variations were observed in the $[Cu\mathbf{L2}]^{2+}$ spectrum for 24 hours at 60 °C.

L1@GNS was prepared by surface exchange on solutions of pegilated GNS and purified with two ultracentrifugation and redissolution cycles. In a typical experiment, 30 mL aqueous solution of pegilated GNS were subdivided in three 10 mL portions. To each of the portions, **L1** was added at 10^{-4}M, 10^{-3}M and 10^{-2} M concentration, and allowed to react for 2 hours. The solutions were then ultracentrifuged and redissolved two times, with supernatant discard, to eliminate excess **L1** molecules. Characterization was carried out by measuring pH, Z potential and absorption spectrum, see Table 3. A red shift of the LSPR maximum was always observed on forming **L1**@GNS from GNS, slightly larger than in the case of $[Cu\mathbf{L1}]^{2+}$, with $\Delta\lambda$ increasing from 12 to 15 nm on increasing the ligand concentration from 10^{-4} to 10^{-2} M (see ESI, Figure S8, for spectra). The pH of the purified **L1**@GNS solutions were weakly acidic, probably as a result of partial protonation (or carbonatation) of the amino groups of **L1** during its synthetic workup. The Z potential is positive in all cases, increasing in the syntheses with more concentrated **L1**, with the charge due to the protonation of the macrocyclic ligand: twelve-membered tetraazamacrocycles bearing all tertiary amines are known to protonate only on two amino groups with logarithmic protonation constants for tetramethyl 12aneN4 of 11.07 and 8.95 (logK1 and logK2, respectively).[42] Very similar values are expected to hold also in the case of **L1**, with the tetraaza rings bis-protonated and bearing a +2 charge at the pH values listed in Table 2. Z vs pH potential titrations on **L1**@GNS also confirm this (ESI, Figure S9), as a decrease of Z to slightly negative values are observed when pH > 11 is reached (neutral ligand situation).

Cu^{2+} was added to the three portions of aqueous **L1**@GNS solution, using a 1:1 molar ratio with respect to the **L1** moles added in the first step. We allowed it to react at 60 °C for 1 hour, replicating the conditions in which full complexation of **L2** is obtained. Z potentials change almost negligibly and within the experimental error, as each macrocyclic unit maintains a +2 charge. The pH values decrease slightly, as a result of H^{+} release from the chelators. The variation of Z potential vs pH of the obtained $[Cu_n(\mathbf{L1}@GNS)]^{2n+}$ products was also tested, finding ~ 10 mV decrease on increasing pH to 10, see Table 3. At this pH, according to what observed with $[Cu\mathbf{L2}]^{2+}$, deprotonation of the copper-coordinated water molecule is complete and the hybrids are to be described as $[Cu_n(OH)_n(\mathbf{L1}@GNS)]^{n+}$, whose reduced charge fits with the decrease of Z potential.

Table 3.Data for the two step approach to the $[Cu_n(\mathbf{L1}@GNS)]^{2n+}$ hybrids

L1 (mol/L) in the grafting reaction	Δλ (nm)	pH	pH after Cu^{2+}	Z (mV)[a]	Z (mV)[a] after Cu^{2+} addition	grafted Cu (mol/L)	average number $[Cu\mathbf{L1}]^{2+}$/ GNS
10^{-4}	12	5.77	5.76	13(4)	14(3) 5(2)[b] pH 10.0	1.5×10^{-6}	500
10^{-3}	13	5.85	5.72	14(4)	14(5) 7(3)[b] pH 10.1	1.9×10^{-6}	760
10^{-2}	15	6.48	5.42	19(5)	16(7) 10(5)[b] pH 9.7	4.0×10^{-6}	1600

[a] values on three different measurements, uncertainties in parenthesis. [b]Z potential remeasured after 0.1M NaOH micro additions up to pH ~ 10 (the effective measured pH is reported in the Table)

It has to be pointed out that complexation reactions were carried out by adding a 1 to 1 Cu^{2+}:ligand amount, with the moles of **L1** calculated as 100% of those added in the displacement reaction. Quantitative grafting of **L1** is of course unlikely in the preceding steps, and the ultracentrifugation cycles were carried out to separate ungrafted **L1** from **L1**@GNS. This means that in the complexation stage some Cu^{2+} remains unreacted. To exactly quantify this, we purified the obtained $[Cu_n(\mathbf{L1}@GNS)]^{2n+}$ with 3 cycles of ultracentrifugation/supernatant discard/redissolution, and analysed Cu^{2+} by oxidation with aqua regia and ICP-OES. Results, summarized in Table 3, show Cu^{2+} concentrations similar to those found when grafting preformed $[Cu\mathbf{L1}]^{2+}$. Moreover, a 100-fold increase of **L1** concentration in the displacement step leads only to a 3-fold increase of the grafted ligand, as calculated by the concentration of their Cu^{2+} complex. From the data of Table 3 it can be seen that only 1.5%, 0.19 % and 0.04% of the added **L1** is grafted on GNS when the PEG-SH displacement reaction is carried out with 10^{-4}M, 10^{-3}M and 10^{-2}M ligand, respectively. Thus, also when void **L1** is grafted, a saturation surface concentration is reached, as it is observed when using preformed $[Cu\mathbf{L1}]^{2+}$. We hypothesize that, in both cases, this might be due to the formation of a positive surface charge on the GNS with the grafting process, that disfavours further grafting of the complex or of the diprotonated free ligand, both bearing a +2 charge.

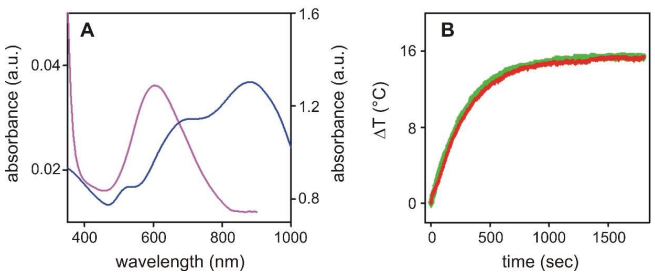

Fig 4 A: absorption spectrum of $[Cu\mathbf{L2}]^{2+}$ at a 5×10^{-4} M concentration in water (purple line, absorbance: left axis) and of pegilated GNS, Au = 3×10^{-4} M (blue line, absorbance: right axis. The purple spectrum is ~ 35 times less intense than the blue one). **B**: thermograms (T increase vs time) obtained on irradiating solutions of pegilated GNS (green points) and of $[Cu_n\mathbf{L1}@GNS]^{2n+}$ (red points) with a laser source at 800 nm (power 200 mW laser waist 2 mm)

In the synthetic approach used in this section, a large amount of the added Cu^{2+} cations remains thus uncomplexed and is eliminated with the purification cycles. Although post-complexation purification techniques are available (*e.g.* radio-HPLC), this would make the preparation procedure less straightforward if a radionuclide of Cu^{2+} have to be used. However, the concentrations of grafted copper listed in Table 3 can be taken as the concentrations of void **L1** that is actually grafted on GNS after the displacement step. Accordingly, we have prepared solutions of **L1**@GNS (with **L1** 10^{-4} M and 10^{-3} M), purified them with two cycles of ultracentrifugation/redissolution, and then we have added 60% of the amount of Cu^{2+} expected to be coordinated in the empty, grafted ligands. After 1 hour reaction at 60 °C, ICP-OES analysis of $[Cu_n(\mathbf{L1}@GNS)]^{2n+}$ after two ultracentrifugation/redissolution cycles showed that all the added Cu^{2+} was coordinated on the GNS surface.

5. Photothermal and Two-Photon Luminescence properties. Although on a different absorbance scale, Figure 4A directly compares the absorption spectrum of $[Cu\mathbf{L2}]^{2+}$ with that of pegilated GNS. The final descending portion of the d-d band of the copper complex at longer wavelengths slightly superimposes to the NIR LSPR band of the GSN. Considering the photothermal properties of GNS, it could be imagined that once the tetraazamacrocyclic complex of Cu^{2+} is grafted on their surface, its d-d band may act as a filter in the radiation absorption and conversion to heat, when using NIR laser sources. However, this is unlikely. With the typical concentration of GNS used in this research (total Au ~ 3.5×10^{-4}M) the absorbance due to the LSPR band is 1.3-1.5 (blue line, right vertical axis in Figure 4A) while that of $[Cu\mathbf{L2}]^{2+}$ at a comparable concentration (10^{-4} M) is only 0.04 on its maximum and 0.015 at 800 nm (purple line, left vertical axis in Figure 4A). Moreover, data in Table 2 and 3 show that the actual concentration of the copper complex, when grafted on GNS, is two orders of magnitude lower than that used to record the spectrum of Figure 4A, i.e. ~ 10^{-6} M, leading to negligible light absorption. This is supposed to have no effect on the photothermal properties of $[Cu_n\mathbf{L1}@GNS]^{2n+}$. We verified it experimentally, by measuring the T increase (ΔT) vs time thermograms obtained irradiating with a 800 nm laser source a solution of pegilated GNS and the same solution after displacement with 10^{-3} M $[Cu\mathbf{L1}]^{2+}$ (green and red points, respectively, in Figure 4B). The two thermograms are superimposable, confirming the prediction. GNS display also remarkable luminescence induced by the sequential absorption of two photons in the NIR region of the spectrum.[43] We have shown[13] that for the GNS type used in this paper, the TPL emission spectrum in aqueous suspension is a broad band in the visible region. While the shape of the TPL emission spectrum is independent on the excitation wavelength, its intensity is governed by the local field enhancement from the plasmon

resonance[44] and reaches its maximum when the excitation source is at a wavelength coincident with the LSPR maximum.[15] On the other hand, Cu(II) complexes are well known to quench fluorescence of molecular fluorophores.[33] To check if any effect is played on TPL emission by the $[Cu\mathbf{L1}]^{2+}$ complexes grafted on the GNS surface, we prepared a 20 mL solution of GNS coated with PEG-SH. The solution was divided in two 10 mL volumes, one was examined as such, measuring the TPL emission spectrum, the second was co-coated with $[Cu\mathbf{L1}]^{2+}$ (10^{-4} M concentration, 60°C) and TPL emission was then measured. We observed perfectly comparable emission spectra (ESI, Figure S10). Moreover, the brightness of $[Cu_n(\mathbf{L1}@GNS)]^{2n+}$ and pegilated GNS has also been obtained by their cross-correlation functions, as it is shown in the ESI. Brightnesses of 8.3 and 8.2 kHz/GNS are calculated from these data for $[Cu_n(\mathbf{L1}@GNS)]^{2n+}$ and pegilated GNS. The values are almost identical and larger than that of the reference Rhodamine 6G (3.4 kHz/molecule), as already found in our previous work for the same GNS type.[16] All the collected data sharply demonstrate that co-coating with $[Cu\mathbf{L1}]^{2+}$ does not influence at all the photothermal properties and the two-photon luminescence of GNS.

Conclusions

The new ligand **L1** has been prepared, equipped with a lipoic acid-terminated arm, allowing its easy grafting on the surface of gold. Addition of **L1** to pegilated GNS gives only partial displacement of PEG-SH, yielding stable, co-coated nanoparticles, **L1**@GNS, that may be easily purified and readily coordinate Cu^{2+} in aqueous solutions, forming the $[Cu_n(\mathbf{L1}@GNS)]^{2n+}$ hybrids. These bear on the surface a comparable number of PEG-SH and of $[Cu\mathbf{L1}]^{2+}$ units, with 600-1600 units of the latter, depending on the preparation conditions. The maximum surface concentration of the copper complex (~1600 $[Cu\mathbf{L1}]^{2+}$/GNS) was obtained by **L1** exchange reaction on pegilated GNS using the ligand in the exceedingly high 10^{-2} M concentration. However, comparable surface co-coating was obtained also using less concentrated **L1** solutions, e.g. 600 $[Cu\mathbf{L1}]^{2+}$/GNS is obtained with 10^{-4}M **L1** in the exchange step, a reassuring result in the perspective of an economical, ligand-saving protocol to produce the desired hybrids. Grafting the copper complex of **L1** on the GNS surface does has no influence on the photothermal and two-photon emission properties of the used GNS. Also the stability of the ligand-Cu^{2+} complex was found remarkable, both towards demetallation at very low pH and towards transmetallation with a series of metal cations typically found *in-vivo*. In our opinion, these results are an excellent proof of concept for the establishment of a suitable synthetic protocol towards the preparation of GNS/Cu^{2+} hybrids, that with ligand **L1,** of different but related strong chelators for Cu^{2+}, could lead to multifunctional nanotools, capable of simultaneous optical TPL tracking and localized photothermal therapy, and also suitable for PET imaging if Cu radionuclides would be used.

Acknowledgements

We thank Fondazione Cariplo Milano, Italy (project 2010-0454) and MIUR (PRIN 2010-2011, 20109P1MH2_003) for funding.

Notes and references

[a]Dipartimento di Chimica, Università di Pavia, viale Taramelli, 12 - 27100 Pavia, Italy;
[b]Institut de Chimie Moleculaire de l'Université de Bourgogne, Université de Bourgogne, UMR CNRS 6302, 9, avenue Alain Savary, 21000 Dijon, France;
[c]Dipartimento di Fisica, Università Milano Bicocca, Piazza della Scienza 3, 20126 Milano, Italy
E-mail: piersandro.pallavicini@unipv.it; Fax (+39)0382 528 544; Tel (+39) 0382 987 336

Electronic supplementary information (ESI) available: Synthesis of GNS and compounds **1-3** and chelator L**3**. Synthesis of activated lipoic acid. Calculation of GNS molar concentration. Spectra relative to aggregation of nude GNS on addition of $[Cu\mathbf{L1}]^{2+}$. TEM images (including those used for measuring average dimensions of GNS and average dimensional parameters taken from them). Transformation yield. Calorimetric profiles (DSC). Details for the calculation of the average number PEG-SH and $[Cu\mathbf{L1}]^{2+}$ per GNS. Absorption spectra for $[Cu\mathbf{L2}]^{2+}$ vs pH. Absorption spectra on addition of void **L1** to pegilated GNS. Z potential vs pH for **L1**@GNS. Brightness calculation
See DOI: 10.1039/b000000x/

1 - E. Boisselier and D. Astruc, *Chem. Soc. Rev.*, 2009**, 38***,* 1759.
2 - M. Shilo, T. Reuveni, M. Motiei and R. Popovtzer, *Nanomedicine* 2012, **7***,* 257.
3 - D. Rand, V. Ortiz, Y. Liu, Z. Derdak, J.R. Wands, M. Tatícek and C. Rose-Petruck, *Nano Lett.*, 2011, **11***,* 2678.
4 - R. Ankri, A. Meiri, S. I. Lau, M. Motiei, R. Popovtzer and D. Fixler, *J. Biophotonics*, 2013, **6**, 188.
5 - W.-S. Kuo, C.-N. Chang, Y.-T. Chang, M.-H. Yang, Y.-H. Chien, S.-J. Chen and C.-S. Yeh, *Angew. Chem. Int. Edit.*, 2010, **49**, 2711.
6 - P. Pallavicini, A. Donà, A. Casu, G. Chirico, M. Collini, G. Dacarro, A. Falqui, C. Milanese, L. Sironi and A. Taglietti, *Chem. Commun.*, 2013, **49**, 6265.
7 - A. Casu, E. Cabrini, A. Donà, A. Falqui, Y. Diaz-Fernandez, C. Milanese, A. Taglietti and P. Pallavicini, *Chem. - Eur. J.*, 2012, **18**, 9381.
8 - P. Pallavicini, G. Chirico, M. Collini, G. Dacarro, A. Donà, L. D'Alfonso, A. Falqui, Y. A. Diaz-Fernandez, S. Freddi, B. Garofalo, A. Genovese, L. Sironi and A. Taglietti, *Chem. Commun*., 2011, **47**, 1315.
9 - H. Yuan, C. G. Khoury, H. Hwang, C. M. Wilson, G. A. Grant and T. Vo-Dinh, *Nanotechnology*, 2012, **23**, 075102.
10 - A. Guerrero-Martínez, S. Barbosa, I. Pastoriza-Santos and L. M. Liz-Marzán, *Curr. Opin. Colloid In.*, 2011, **16***,* 118.
11 – P. Pallavicini, A. Donà, A. Taglietti, P.Minzioni, M. Patrini, G. Dacarro, G. Chirico, L. Sironi, N. Bloise, L. Visai and L. Scarabelli, *Chem. Commun.*, 2014, **50**, 1969.
12 - H. Yuan, A. M. Fales and T. Vo-Dinh, *J. Am. Chem. Soc.*, 2012, **134**, 11358.
13 - G. Chirico, M. Collini and P. Pallavicini, *Nanomedicine*, 2014, **9**, 1.
14 – D. H. M. Dam, J. H. Lee, P. N. Sisco, D. T. Co, M. Zhang, M. R. Wasielewski and T. W. Odom, *ACS Nano*, 2012, **6**, 3318.
15 - L. Sironi, S. Freddi, M. Caccia, P. Pozzi, L. Rossetti, P. Pallavicini, A. Donà, E. Cabrini, M. Gualtieri, I. Rivolta, A. Panariti, L. D'Alfonso, M. Collini and G. Chirico, *J. Phys. Chem. C*, 2012, **116**, 18407.
16 - G. Cavallaro, D. Triolo, M. Licciardi, G. Giammona, G. Chirico, L. Sironi, G. Dacarro, A. Donà, C. Milanese and P. Pallavicini, *Biomacromolecules*, 2013, **14**, 4260.

17 – F. Manea, F. Bodar Houillon, L. Pasquato and P. Scrimin, *Angew. Chem. Int. Edit.*, 2004, **43**, 6165.
18 - M. Diez-Castellnou, F. Mancin and P. Scrimin, *J. Am. Chem. Soc.*, 2014, **136**, 1158.
19 - P. D. Beer, D. P. Cormode and J. J. Davis, *Chem. Commun.*, 2004, 414.
20 - S. Sung, H. Holmes, L. Wainwright, A. Toscani, G. J. Stasiuk, A. J. P. White, J. D. Bell and J. D. E. T. Wilton-Ely, *Inorg. Chem.*, 2014, **53**, 1989.
21 - M. F. Ferreira, B. Mousavi, P. M. Ferreira, C. I. O. Martins, L. Helm, J. A. Martins and C. F. G. C. Geraldes, *Dalton T.*, 2012, **41**, 5472.
22 - X. Sun, R. Rossin, J. L. Turner, M. L. Becker, M. J. Joralemon, M. J. Welch and K.L. Wooley, *Biomacromolecules*, 2005, **6**, 2541.
23 - A. I. Jensen, T. Binderup, P. E. K. Kumar, A. Kjær, P. H. Rasmussen and T. L. Andresen, *Biomacromolecules*, 2014, **15**, 1625.
24 - C. Tu, X. Ma, A. House, S. M. Kauzlarich and A. Y. Louie, *ACS Med. Chem. Lett.*, 2011, **2**, 285.
25 - K. Chen, Z.-B. Li, H. Wang, W. Cai and X. Chen, *Eur. J. Nucl. Med. Mol. I.*, 2008, **35**, 2235.
26 - B. R. Jarrett, B. Gustafsson, D. L. Kukis and A. Y. Louie, *Bioconjugate Chem.*, 2008, **19**, 1496.
27 - J. Xie, K. Chen, J. Huang, S. Lee, J. Wang, J. Gao and X. Li, *Biomaterials*, 2010, **31**, 3016.
28 - H.-Y. Lee, Z. Li, K. Chen, A. R. Hsu, C. Xu, J. Xie, S. Sun and X. Chen, *J. Nucl. Med.*, 2008, **49**, 1371.
29 – Y. Wang, Y. Liu, H. Luehmann, X. Xia, P. Brown, C. Jarreau, M. Welch and X. Xia, *ACS Nano*, 2012, **6**, 5880.
30 - X. Liu, M. Yu, H. Kim, M. Mameli and F. Stellacci, *Nature*, 2012, **3**, 1182.
31 - R. H. Terrill, T. A. Postlethwaite, C.-H. Chen, C.-D. Poon, A. Tarzis, A. Chen, J. E. Hutchison, M. R. Clark, G. Wignall, J. D. Londono, R. Superfine, M. Flavo, C. S. Johnson Jr., E. T. Samulski and R. W. Murray, *J. Am. Chem. Soc.*, 1995, **117**, 12537.
32 - O. Kohlmann, W. E. Steinmetz, X.-A. Mao, W. P. Wuelfing, A. C. Templeton, R. W. Murray and C. S. Johnson Jr., *J. Phys. Chem. B*, 2001, **105**, 8801.
33 - L. Fabbrizzi, M. Licchelli and P. Pallavicini, *Acc. Chem. Res.*, 1999, **32**, 846.
34 - S.-Y. Lin, Y.-T. Tsai, C.-C. Chen, C.-M. Lin and C.-H. Chen, *J. Phys. Chem. B*, 2004, **108**, 2134.
35 - J. M. Abad, S. F. L. Mertens, M. Pita, V. M. Fernàndez and D. J. Schiffrin, *J. Am. Chem. Soc.*, 2005, **127**, 5689.
36 - S. Roux, B. Garcia, J.-L. Bridot, M. Salomé, C. Marquette, L. Lemelle, P. Gillet, L. Blum, P. Perriat and O. Tillement, *Langmuir*, 2005, **21**, 2526.
37 - A. Aqil, S. Vasseur, E. Duguet,;C. Passirani, A. Roch, R. Muller, R. Jerome and C. Jerome, *Eur. Polym. J.*, 2008, **44**, 3191.
38 - A. Vonarbourg, C. Passirani, P. Saulnier, P. Simard, J. P. Leroux and J. P. Benoit, *J. Biomed. Mater. Res. A*, 2006, **78A (3)**, 620.
39 - H. Elias, *Coord. Chem. Rev.*, 1999, **187**, 37.
40 - F. Denat, Y. A. Diaz-Fernandez, L. Pasotti, N. Sok and P. Pallavicini, *Chem. - Eur. J.*, 2010, **16**, 1289.
41 - M. C. Styka, R. C. Smierciak, E. L. Blinn, R. E. De Simone and J. V. Passariello, *Inorg. Chem.*, 1978, **17**, 82.
42 - R. D. Hancock, P. W. Wade, M. P. Ngwenya, A. S. de Sousa and K. V. Damu, *Inorg. Chem.*, 1990, **29**, 1968.
43 - P. Biagioni, M. Celebrano, M. Savoini, G. Grancini, D. Brida, S. Mátéfi-Tempfli, M. Mátéfi-Tempfli, L. Duò, B. Hecht, G. Cerullo and M. Finazzi, *Phys. Rev. B*, 2009, **80**, 045411.
44 - D. S. Wang, F. Y. Hsu and C. W. Lin, *Opt. Express*, 2009, **17**, 11350.